This is an open access article published under an ACS AuthorChoice License, which permits copying and redistribution of the article or any adaptations for non-commercial purposes.

THE JOURNAL OF PHYSICAL CHEMISTRY B

Article

pubs.acs.org/JPCB

Excited State Proton Transfer of Natural Flavonoids and Their Chromophores in Duplex and Tetraplex DNAs

Bidisha Sengupta,*[,†] Samantha M. Reilly,[‡] Donald E. Davis, Jr.,[†] Kisa Harris,[†] Randy M. Wadkins,[‡] Denise Ward,[†] D'Asia Gholar,[†] and Cari Hampton[†]

[†]Department of Chemistry, Tougaloo College, Tougaloo, Mississippi, 39174, United States

[‡]Department of Chemistry and Biochemistry, University of Mississippi, University, Mississippi, 38677, United States

Supporting Information

ABSTRACT: Fisetin (3,7,3′,4′-tetrahydroxyflavone) and quercetin (3,5,7,3′,4′-pentahydroxyflavone) are the bioactive plant flavonoids that are potentially useful therapeutic drugs for the treatment of a broad spectrum of diseases, including atherosclerosis, cardiovascular disease, obesity, hypertension, and cancer. 3-Hydroxyflavone (3HF) and 7-hydroxyflavone (7HF) are the synthetic chromophores of fisetin and quercetin. We have exploited dual luminescence properties of fisetin and quercetin along with 3-HF and 7HF to examine their efficacy of binding and compare their interactions with DNA, which is one of the macromolecular targets of flavonoids in physiological systems. Following the sequence of the human telomeric DNA 5′-d(CCCTAA-)$_n$/(-TTAGGG)$_n$-5′, two single-stranded DNA oligonucleotides, 5′-d$(C_3TA_2)_3C_3$-3′ and 5′-d$(T_2AG_3)_4$-3′, and their duplex were used as receptors to study binding by the ligands quercetin, fisetin, and their chromophores. Circular dichroism, differential absorption, UV thermal melting, and size exclusion chromatographic studies indicated the formation of unusual DNA structures (such as C_4 and G_4 tetraplexes) for both the C- and G-rich single-stranded DNAs. Upon binding to DNA, dramatic changes were observed in the intrinsic fluorescence behavior of the flavonoids. Molecular docking studies were performed to describe the likely binding sites for the ligands. The spectroscopic studies on flavonoid−DNA interactions described herein demonstrate a powerful approach for examining their DNA binding through exploiting the highly sensitive intrinsic fluorescence properties of the flavonoids as their own "reporter" for their interactions with macromolecular targets.

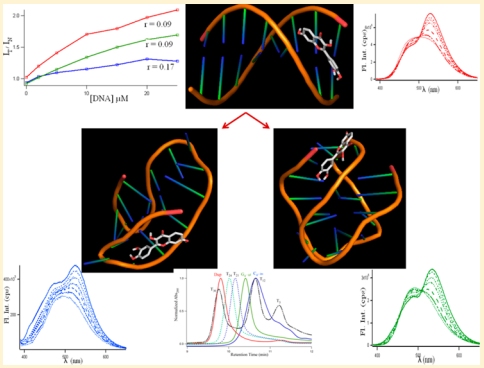

INTRODUCTION

Flavonols and related plant products of the flavonoid group are in prominence from a biomedical context for their wide range of therapeutic activities of high potency and low systemic toxicity.[1] Rusznyák and Szent-Györgyi first drew attention to the therapeutically beneficial role of dietary flavonoids.[2] Flavonoids are abundant in common plant-based foods and beverages, such as onions, apples, berries, tea, and red wine. The Western European diet contains, on average, ∼3−58 mg of flavonoids per day.[3] The French paradox[4] (first noted by the Irish physician Samuel Black in 1819) refers to the fact that the French suffer relatively low incidence of coronary heart disease because their diet is rich in both saturated fats and red wine (with high flavonoid content). Both in vivo and in vitro studies show that flavonoids are therapeutically effective against a wide range of diseases, including cancers, allergies, AIDS, and different free-radical-mediated disorders, such as atherosclerosis, ischemia, neuronal degeneration, and cardiovascular ailments etc.,[4,6−8] which make them promising alternatives to conventional therapeutic drugs.

The possible target molecules and the mode of interactions between flavonoids and their targets are the subject of ongoing research, but it is known that single- and double-stranded nucleic acids structures can serve as receptors for flavonoids.[9,10] The interactions of small molecules with nucleic acids are of considerable interest for the design of novel therapeutically important compounds that are effective against cancer, heart disease, and other physiological and neurological disorders.[4−8,11] Although the duplex is the most common arrangement of DNA, the terminal part of the telomeric DNA is G-rich and single-stranded.[12] Although the precise repeats of the sequence CCCTAA/TTAGGG[13] form a classical Watson−Crick double helix, the individual single G-rich and C-rich telomeric strands can form unusual DNA structures under appropriate conditions. The G-rich strand can form a four-stranded G-quadruplex structure involving planar G-quartets, and the C-rich strand can form the so-called tetraplex i-motif structure with intercalated C·C$^+$ base pairs[14−16] (Scheme 1). Formation of unusual, non-B DNA structures in specific

Special Issue: Photoinduced Proton Transfer in Chemistry and Biology Symposium

Received: August 25, 2014
Revised: October 27, 2014
Published: November 13, 2014

 © 2014 American Chemical Society dx.doi.org/10.1021/jp508599h | J. Phys. Chem. B 2015, 119, 2546−2556

Scheme 1. Structures of (a) G-Quartet; (b) C·C$^+$ Hemiprotonated Base Pair; (c) Duplex Base Pairing between Guanine (G)-Cytosine (C) and Adenine (A)-Thymine (T); (d) 3-Hydroxyflavone (3HF); (e) 7-Hydroxyflavone (7HF); (f) Fisetin; and (g) Quercetin

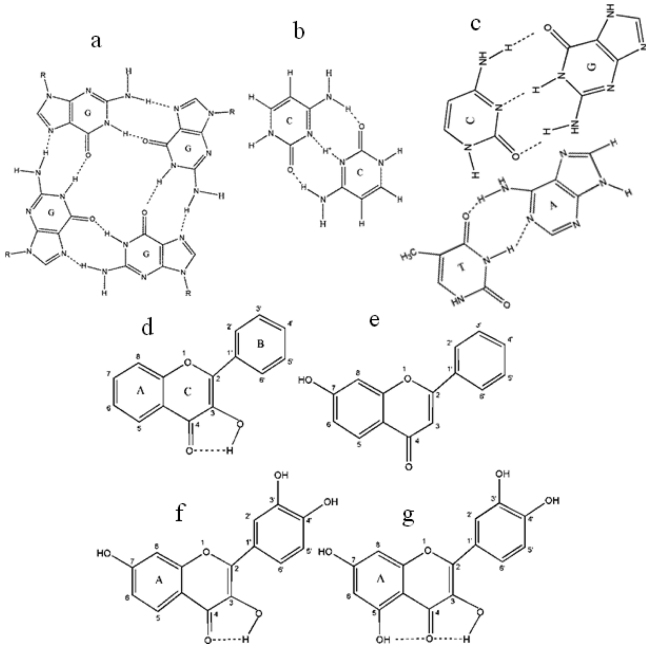

sequential motifs is thought to take place during various physiological processes (e.g., some quadruplex formation was evidenced throughout the cell cycle).[17] Human telomeric DNA and proto-oncogenes have the higher potential to form G_4 DNA compared with tumor-suppressor genes,[18] suggesting the possibility of treating cancer cells distinctively with effective G_4 ligands. This opens the door to small-molecule targeting of telomeric G_4 in cancer therapy because small molecules can trap quadruplex structures.[19]

In this article, we provide results of a systematic study on two therapeutically important flavonols, fisetin (3,7,3′,4′−OH flavone) and quercetin (3,5,7,3′,4′−OH flavone), and their chromophores, 3-hydroxyflavone (3HF) and 7-hydroxyflavone (7HF), in three types of DNA matrices: duplex DNA, the C_4 intercalated motif (i-motif), and the G_4 quadruplex made from 5′-d$(C_3TA_2)_3C_3$-3′ and 5′-d$(T_2AG_3)_4$-3′ oligonucleotides. Recently,[20] we have shown that fisetin is an effective G_4 quadruplex ligand. Fisetin and quercetin are the most abundant dietary flavonoids,[21] (widely present in strawberries, apples, onions, broccoli, and many other fruits and vegetables) and belong to the most commonly occurring chemical class of flavonoids; namely, flavonol. Quercetin binds to human plasma proteins and inhibits the activities of enzymes, including kinases[22] and DNA topoisomerases.[23] Fisetin inhibits protein kinase C, a signal transducing enzyme,[24] and HIV-1 proteinase,[25] a virally encoded protein that is indispensable for the maturation and processing of the AIDS virus. It also exhibits strong antioxidant properties in membrane environments[26] and has also been found to be effective in preventing nonenzymatic glycosylation of hemoglobin.[27] Flavones consist of two aromatic rings (rings A and B) linked through a pyrone (ring C) (see Scheme 1).

Here, we demonstrate how fluorescence spectroscopy is an exquisitely sensitive tool for noninvasive sensing of DNA-flavonoid interactions at physiologically relevant conditions via measurements of steady state emission parameters of the intrinsic fluorescence of the ligand (flavonoid) in the target (DNA) environment. The high qualitative and quantitative sensitivity of fluorescence provides enormous advantages when compared with most other physical techniques and offers a powerful approach for detection of nucleic acid−flavonoid interactions at physiologically relevant concentrations (10^{-6} M). We highlight novel applications of the remarkably environmentally sensitive "two-color" fluorescence exhibited by two important flavonoids, which permits multiparametric and ratiometric measurements. To consolidate findings obtained via fluorescence spectroscopy, results from other relevant experimental biophysical techniques of related interest (circular dichroism (CD), differential absorption, UV thermal melting, size exclusion chromatography (SEC)), and molecular modeling are also discussed here.

MATERIALS AND METHODS

The flavonoids fisetin, quercetin, 3HF, and 7HF and oligonucleotides 5′-d$(C_3TA_2)_3C_3$-3′ and 5′-d$(T_2AG_3)_4$-3′ were purchased from the Sigma-Aldrich Chemical Co. and Integrated DNA Technologies, respectively, and were used as obtained. The solvents used were of spectroscopic grade and checked for any absorbing or fluorescent impurities. Stock solutions of 3HF, 7HF, fisetin, and quercetin were prepared in ethanol (because of low solubility in an aqueous system), and the final experimental concentrations of all flavonoids were kept on the order of 10^{-6} M, ethanol <1% (v/v). The desalted oligonucleotides were dissolved in deionized water. For G- and C-rich oligonucleotides, 10 mM Tris−HCl at pH 7.4 and 10 mM sodium citrate at pH 6 buffers were used, respectively. The duplex DNA was made by dissolving equimolar concentrations of the G- and C-rich oligonucleotides in 10 mM pH 7.0 citrate buffer. For some experiments with the G-rich DNA, 10 mM, pH 7.0 citrate buffer was also used, and it is pertinent to mention that there was no major difference in the spectral features of single-stranded and duplex DNAs between Tris−HCl, pH 7.0 and citrate, pH 7.0 buffers. The UV thermal melting and differential absorption studies were performed in 10 mM Tris−HCl, 100 mM NaCl, pH 7.2 for G-rich DNA, whereas 10 mM citrate, 100 mM $NaClO_4$, pH 6.0, was used for C-rich, and pH 7, for duplex DNAs.

Steady state absorption spectra were recorded with Shimadzu UV 2550 spectrophotometers with a Peltier temperature controller and 8-microcell holder accessories were used for melting studies, with 1 °C/min and a wait period of 240 s. Steady state fluorescence measurements were carried out with a Fluoromax-4 (Horiba Jobin Yvon) spectrofluorometer equipped with polarizers and a Peltier temperature-controlled cell.

Steady state fluorescence anisotropy (**r**) values were calculated using the expression

$$\mathbf{r} = \frac{I_{VV} - GI_{VH}}{I_{VV} + 2GI_{VH}} \quad (1)$$

where I_{VV} and I_{VH} are the vertically and horizontally polarized components of the flavonoid emission after excitation by vertically polarized light at the respective wavelength. G is the sensitivity factor of the detection systems.[28]

Circular dichroism spectra were acquired with a J-710 spectropolarimeter (Jasco). The scan rate was 50 nm/min, and three consecutive spectra were averaged to produce the final

dx.doi.org/10.1021/jp508599h | J. Phys. Chem. B 2015, 119, 2546−2556

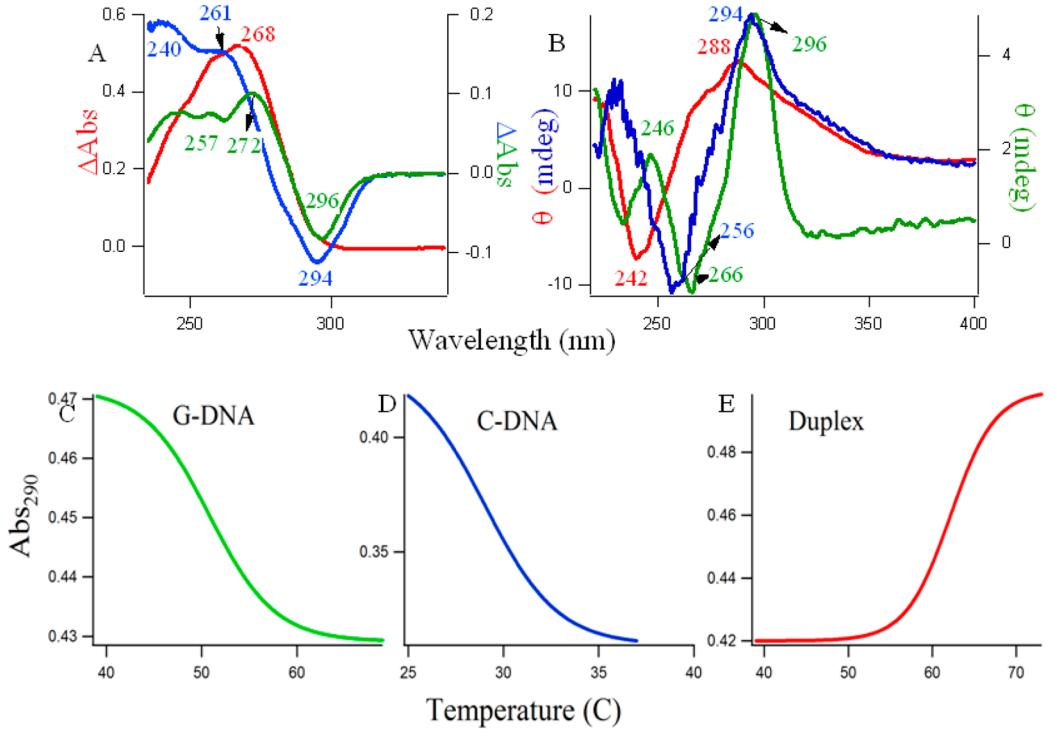

Figure 1. (A) Thermal difference spectra of 5 μM DNAs; (B) circular dichroism spectra of 5−10 μM DNAs; (C) typical UV melting profiles. Blue and green lines denote single-stranded C_4 and G_4 at pH 6.0 and 7.0, respectively; and the red line indicates the duplex DNA made of the complementary sequences at pH 7.0.

spectrum. All spectral measurements were performed at 25 °C. The highest concentration of DNA for fluorescence and circular dichroism experiments were kept at ∼20−25 μM to avoid aggregation, scattering, and artifacts.

SEC used a 300 × 7.8 mm i.d. column (BioSep, 3000, Phenomenex) on an HPLC system (SCL 10A VP, Shimadzu) using a 10 mM citrate buffer at pH 6.5 with 100 mM $NaClO_4$ to minimize matrix adsorption.[29] For the thymine oligonucleotides dT_5, dT_{12}, dT_{21}, dT_{24}, and dT_{30}, the averages of the retention times and the corresponding molecular masses were fitted linearly, from which the folded nature of the 5′-$d(C_3TA_2)_3C_3$-3′ and 5′-$d(T_2AG_3)_4$-3′ DNA were determined, assuming that there were no secondary interactions within the thymine oligonucleotides. Here, the molar masses of the thymine oligonucleotides were used as standards for drawing a calibration plot to obtain the molecular masses of the free and bound DNAs for stoichiometric purposes. Absorption and fluorescence measurements of the species were made using the SPD-10AVi and RF-10AXL Shimadzu detectors, respectively. The time difference between the two detectors was determined from the absorption (260 nm) and the emission (λ_{ex} = 307 nm, λ_{em} = 370 nm) using the oligonucleotide 5′-CAGC/2AmPr/GCAG-3′, where 2AmPr is 2-aminopurine. The injection volume was 20 μL. Three or more chromatographs were acquired to determine an average retention time.

All computer docking studies were performed using Autodock 4.2 following the general protocols already in place.[30,31] The structures of fisetin, quercetin, 3HF, and 7HF were created using ChemBioDraw Ultra v. 13.0 (CambridgeSoft Corporation, Cambridge, USA) and were then energy-minimized using UCSF Chimera.[32] These structures were then loaded into AutoDockTools4.[30] The DNA structures of an antiparallel quadruplex (RCSB PDB 143D),[33] an antiparallel i-motif (RCSB PDB 1A83),[34] and an A-DNA sequence (RCSB PDB 173D)[35] were used as targets. The duplex DNA was made using a Python program based on the B-DNA coordinates provided by Arnott and Hukins.[36] For the AutoGrid4 module of AutoDockTools4, grid volumes were optimized for each DNA to ensure that the entire DNA was available for docking. Once the grid was created, 10 Lamarckian general algorithms (GA) were performed on the molecules, with each DNA with a population size of 150 and a limit of 2.5 million energy evaluations. All other parameters were left at the default settings originally loaded into AutoDockTools4. The lowest energy conformations for each molecule docked to each unique DNA structure were then selected. The PyMOL software package was used for visualization of the docked conformations.

RESULTS AND DISCUSSIONS

Circular Dichroism, UV Melting and Thermal Differential Absorption Spectroscopy. The UV absorption of the fisetin- and quercetin-bound nucleic acids from 200 to 300 nm is shown in Supporting Information (SI) Figure S1A,B), which is due to the transitions of the planar purine and pyrimidine bases.[37] The λ_{abs}^{max} of $d(C_3T_2A)_3C_3$ in pH 6.0, $d(T_2AG_3)_4$ in pH 7.0, and duplex DNA in pH 7.0 are ∼265, 255, and 258 nm, respectively, which suggests the difference in inpacking of DNA bases in these DNAs as well as confirms[37] that the overall secondary structures dictate the absorption spectra. The absorption spectra of fisetin and quercetin in different environments are displayed in the SI Figure S1A,B insets, where it is observed that λ_{abs}^{max} of fisetin is 360, 361, and 366 nm, and quercetin is ∼368, 380, and 376 nm in $(C_3T_2A)_3C_3$ and $(T_2AG_3)_4$, duplex DNAs and 357 and 362 nm for fisetin and 369 and 373 nm for quercetin in pH 6.0 and pH 7.0 buffers, respectively. The changes in λ_{abs}^{max} between buffers and DNA

dx.doi.org/10.1021/jp508599h | J. Phys. Chem. B 2015, 119, 2546−2556

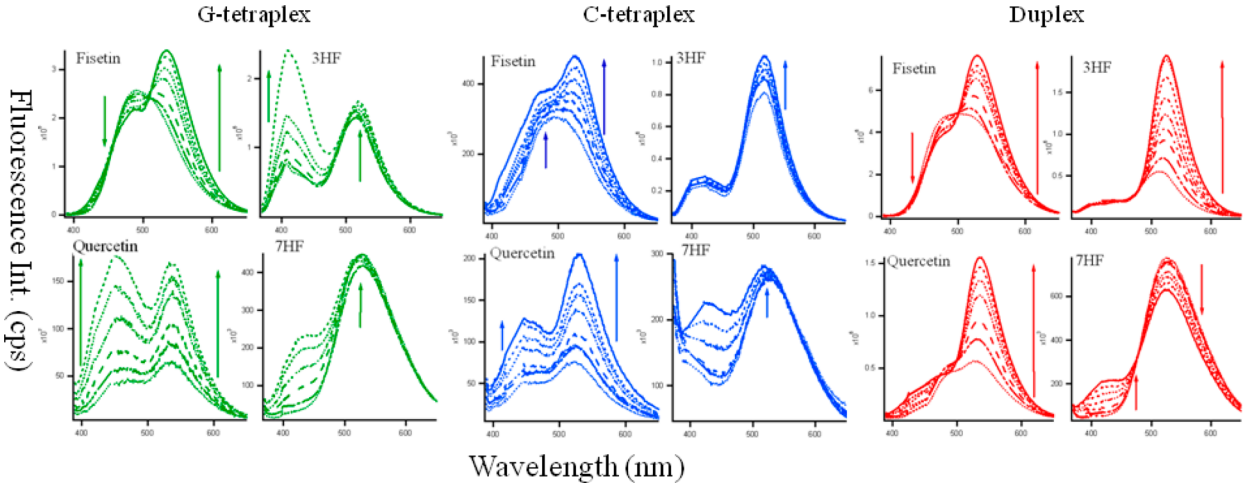

Figure 2. Fluorescence emission spectra of fisetin (λ_{ex} = 370 nm), quercetin (λ_{ex} = 370 nm) 3-hydroxyflavone (3HF, λ_{ex} = 350 nm) and 7-hydroxyflavone (7HF, λ_{ex} = 350 nm) (all ~10 μM) in the presence of increasing concentration of G_4 (green), C_4 tetraplex (blue), and duplex DNA (red) at ~0–25 μM), (0····, 2 – - - –, 5 – – –, 10 —·—·—, 15 —·—·—, 20 - - -, 25 — μM). Slit widths were 3,3 for 3HF and fisetin and 3,5 for quercetin and 7HF.

environments for fisetin and quercetin suggest the binding of flavonols with the DNA.

Figure 1 provides the evidence of the formation of the unusual non-Watson–Crick type of structures for the single-stranded $d(C_3T_2A)_3C_3$ and $d(T_2AG_3)_4$ DNAs at pH 6.0 and 7.0, respectively. Figure 1A shows the thermal difference spectra[37−40] and the corresponding thermal denaturation at 290 nm (Figure 1C,D,E) of the different DNAs, where green, blue, and red lines represent $(C_3T_2A)_3C_3$ at pH 6.0, $(T_2AG_3)_4$ at pH 7.0, and a duplex of the equimolar mixture of the above DNAs in pH 7.0, respectively. The curves in Figure 1A are simply the result of the arithmetic difference between high (90 °C) and low temperature (20 °C) absorption spectra. These spectra provide information complementary to circular dichroism.[37] In Figure 1A, the spectral profile for G-rich DNA (green line) showed two positive maxima at ~244 and 272 nm, a shoulder at 257 nm, and a negative minimum at 296 nm. The C-rich DNA (blue line) showed two positive maxima at ~240 and 261 nm and a negative minimum at 294 nm. The duplex DNA (red line) has a positive maximum at 268 nm. Differential absorption spectra have a typical and unique shape for C i-motifs and G quadruplexes,[37−40] and the characteristics of the spectral profile observed here are clearly supportive of the formation of C_4 intercalated tetraplex (see Scheme 1B), G_4 quadruplexes (see Scheme 1A), and duplex (see Scheme 1C), respectively.

SI Figure S2 shows the differential absorption spectra of the $d(C_3T_2A)_3C_3$ and $d(T_2AG_3)_4$ oligonucleotides in 10 mM citrate buffers of various pHs (5.0, 5.5, 6.0, 6.5, 7.0), and it is observed that the pH 6.0 and 7.0 were the optimum pHs (closest to physiological pH) for C_4 i-motif and G_4 quartet structures to be formed. Hence, all further studies were performed in those pHs. Figure 1B shows the CD spectra of three different DNA molecules made of single-stranded $d(C_3T_2A)_3C_3$ (blue solid line), single-stranded $d(T_2AG_3)_4$ (green solid line), and the duplex of both (red solid line). From here on, the term C_4 and G_4 will be used for $d(C_3T_2A)_3C_3$ and $d(T_2AG_3)_4$ DNAs, respectively. CD spectra provide diagnostic signatures for the structures of intercalated C_4, G_4 quartet, and duplex DNA. Natural, heterogeneous DNA usually adopts the B DNA form, which provides a conservative CD spectrum with small amplitude bands: a positive band around 280–290 nm and a negative one at ~240–145 nm.[37−40] The characteristic CD spectrum of the C_4 i-tetraplex contains a large maximum, ~290 nm; a negative band, ~265 nm; and another small positive band, ~225 nm.[37−40] On the other hand, a positive peak around 260 nm and a trough around 240 nm implies the presence of a parallel G-quadruplex structure, and a peak around 295 nm with a trough around 260 nm generally implies an antiparallel G-quadruplex.[37−40] The distinctive green, blue, and red CD spectral profiles in Figure 1B readily match with the signatures of antiparallel G_4, C_4 i-motif, and duplex DNA, respectively, indicating the existence of these structures under our experimental conditions. Figure 1C,D,E are the thermal melting profiles of the G, C, and duplex DNA molecules studied at the absorption wavelength of 290 nm. The considerable hypochromic shift at 290 nm with increasing temperature in Figure 1C,D were indicative of quadruplex structures,[37] and the midpoints of the melting transitions provide the melting temperature, T_m. The increase in the absorption with an increase in the temperature in Figure 1E follows the normal denaturation profile of a duplex DNA. The T_m values for G_4, C_4, and duplex DNAs were 30, 51, and 62 °C respectively.

Steady State Fluorescence Spectroscopy. Large Stokes-shifted emissions with distinctive fluorescence signatures are obtained for fisetin, quercetin, and the chromophore 3HF when mixed with DNA, indicating their binding with the DNA molecules. In DNA environments, these flavonoid molecules exhibit photoinduced, excited state intramolecular proton transfer (ESIPT), resulting in "two-color" (in the blue-violet and yellow-green regions) fluorescence, the relative contributions between the two colors being strongly modulated by the local environment of the fluorophores.

Figure 2 presents the fluorescence emission spectra of the natural flavonoids (fisetin and quercetin; see Scheme 1f,g) along with the synthetic chromophores 3HF and 7HF (see Scheme 1d,e) with increasing concentrations of G_4 (green), C_4 (blue), and the duplex (red) DNAs. It is evident that addition of DNA induces drastic changes in the emission behavior of the flavonoids. In an aqueous medium, the fluorescence spectra of fisetin exhibit strong overlap between the normal and tautomer

dx.doi.org/10.1021/jp508599h | J. Phys. Chem. B 2015, 119, 2546–2556

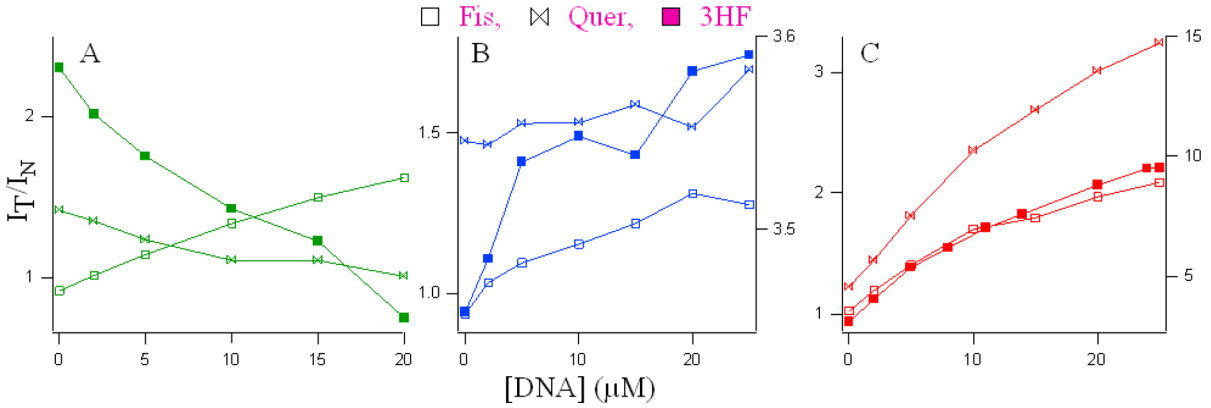

Figure 3. Variation of the I_T/I_N values for flavonoids with increase in DNA concentration from 0 to 25 μM. Green, blue, and red profiles denote G_4, C_4, and duplex DNAs, respectively.

emission bands.[41] With the addition of the G_4, dual fluorescence behavior is observed.

The emission spectra of fisetin consist of two-color-fluorescence bands; namely, a yellow-green emission band along with a high-energy band in the blue-violet region. The blue-violet fluorescence is assigned to the S_1 ($\pi\pi^*$) → S_0 normal (N, nonproton transferred) emission. The large-Stokes shifted green fluorescence is attributed to emission from a tautomer (T) species generated by an excited state intramolecular proton transfer process occurring along the internal H-bond (C(4)═O···HO−C(3)) of the molecule (Scheme 1D,F).[41] The blue-violet and yellow-green fluorescence emissions occur from N* and T* species, respectively.

With the increase in G_4, there is a decrease in the normal emission, with an increase in the tautomer emission. The intensity ratio of tautomer and normal fluorescence (I_T/I_N) increases rapidly with increasing G_4 (shown in Figure 3A) until ~20 μM. The intramolecular H-bond of fisetin, which permits the ESIPT process, was enhanced in the presence of G_4 DNA. It is noteworthy that the emission profiles of fisetin recorded in the DNA solutions resemble the situation in an aprotic environment where ESIPT emission behavior is prominent.[42] The enhanced tautomer emission as well as the strongly red-shifted (~18 nm for tautomer from 0 (516 nm) to 25 μM DNA (534 nm)) fluorescence band indicate that the guest (fisetin) molecules experience relatively aprotic environments (e.g., like solvent acetonitrile, λ_{em}^{max} = 536 nm)[26,42] in the DNA microenvironment (see Figure 2, Table 1). This establishes fisetin as an excellent two-color fluorescent probe to study its microenvironment. Table 1 summarizes the fluorescence emission parameters: λ_{em}^{max} of the ESIPT species and the I_T/I_N (ratio of fluorescence intensities of tautomer and normal ratio) of the natural flavonoids fisetin, quercetin, 3HF, and 7HF in all the DNA solutions.

Flavonols (flavonoids with a 3-OH group) undergo ultrafast photoinduced ESIPT reaction (via the intramolecular hydrogen bond between the C═O and 3-OH groups), which results in the transformation of the initially excited (N*) state to the tautomer (T*) form.[26,41−43] This leads to two-color fluorescence, in the blue-violet and yellow-green regions, which originates from the N* and T* states, respectively. Although the blue-violet fluorescence is assigned to the S_1 ($\pi\pi^*$) → S_0 normal (nonproton-transferred) emission, the large Stokes-shifted green fluorescence is attributable to emission from a tautomer species generated by an excited state intramolecular proton transfer (ESIPT) process occurring

Table 1. Fluorescence Emission Wavelengths (λ_{em}^{max}) of the ESIPT Species along I_T/I_N[a] of 3-Hydroxyflavone (3HF), 7-Hydroxyflavone (7HF), Fisetin, Quercetin in the C_4 i-motif, G_4 Quadruplex, and Duplex DNAs

emission parameters	C_4 i-motif (in pH 6)	antiparallel G_4 (in pH 7)	duplex (in pH 7)	buffer
3-HF				
λ_{em}^{max}(nm)	518	520	526	514,[b] 518[c]
I_T/I_N	3.59	0.75	9.5	2.8,[b] 3.5[c]
7-HF				
λ_{em}^{max}(nm)	518	523	525	526,[b] 525[c]
fisetin				
λ_{em}^{max}(nm)	526	534	529	516,[b] 514[c]
I_T/I_N	1.28	1.79	2.09	1.0,[b] 0.94[c]
quercetin				
λ_{em}^{max} (nm)	530	535	536	529,[b] 523[c]
I_T/I_N	1.7	1.01	3.24	1.3,[b] 1.47[c]

[a]Ratio of fluorescence intensities of tautomer: normal. [b]In pH 7. [c]In pH 6. I_T/I_N could not be obtained because of the insignificant presence of the normal form of 7HF in buffer and low concentrations of DNA. λ_{ex} = 370 nm for fisetin and quercetin and 350 nm for 3HF and 7HF, respectively. For I_T/I_N, fluorescence intensities were observed at 530 nm for tautomer species for all the flavonoids, 470 nm for normal species for quercetin and fisetin, and 430 nm for the normal species of 3HF.

along the internal H-bond (i.e., C(4) = O···HO−C(3)) of the molecule (Scheme 1 G).[41−43] The ESIPT process in flavonols is remarkably sensitive to the external hydrogen-bonding interference of the environment on the internal hydrogen bond of the molecules, and consequently, the relative contribution between the two colors is strongly modulated by the local environment of the fluorophore. In the case of flavonols in which 5-OH and 3-OH groups are simultaneously present (e.g., quercetin), the C(4)═O···HO−C(5) hydrogen bond interferes with the C(4)═O···HO−C(3) hydrogen bond, thus preventing efficient ESIPT[44,45] (see Scheme 1). This results in low fluorescence quantum yield in free states. However, strong fluorescence signals are observed upon binding to a target or in rigid environments.[44,45]

We observed a similar situation for quercetin binding in duplex DNA where a 2.9-fold increase in the ESIPT emission took place. Binding of quercetin with duplex DNA disrupts the

dx.doi.org/10.1021/jp508599h | J. Phys. Chem. B 2015, 119, 2546−2556

internal hydrogen bond involving the 5-OH group, thereby facilitating the ESIPT process.[45] Interestingly, for quercetin, I_T/I_N decreases from 1.42 in buffer (λ_{em}^{max} = 530 nm) to 1.01 (λ_{em}^{max} = 535 nm) in 20 μM G_4 DNA. Similarly, for 3HF, there is a simultaneous increase of the normal and tautomer emission, with a tautomer red shift from 514 (in buffer, I_T/I_N = 2.73) to 520 nm (in 20 μM G_4, I_T/I_N = 0.75) (Figure 1, green spectra). The tautomer of 7HF undergoes a blue shift from 526 to 523 nm with a slight increase in its intensity, and the normal species (absent in buffer) grew significantly in G_4 solutions.

SI Figure S3 displays the excitation spectra of the flavonoids (monitored for the PT fluorescence) in buffer and 20 μM G_4 DNA, where an appreciable change in the spectral profiles was observed. The λ_{ex}^{max} changes from 339 → 343 nm (more polar) and 370 → 365 nm (more aprotic) from buffer to 20 μM G_4 in 3HF and quercetin, respectively. There is an increase in the intensity of the excitation spectra of fisetin between buffer and G_4 DNA. It is pertinent to mention that fluorescence excitation spectra look at the excited state of the chromophore; hence, a change in the excitation spectra clearly indicates that the microenvironments of flavonoids predominantly change in DNA solutions (see Figures 2, 3 and Tables 1, 2).

Table 2. Binding Parameters[a] for the Flavonoids in C_4 i-Motif, G_4 Quadruplex, and Duplex DNAs, Obtained from Experimental Data

binding parameters	C_4 i-motif	antiparallel G_4	duplex	buffer
3-HF				
K_a (M^{-1})	8.8×10^4	6.38×10^4	8.67×10^4	
r	0.09	0.09	0.09	
ΔG^0(kcal/mol)	−6.74	−6.55	−6.73	
7-HF				
r	0.09	0.05	0.05	0.04
fisetin				
K_a (M^{-1})	1.65×10^{05}	2.2×10^4	4.62×10^4	0.03
r	0.17	0.09	0.09	
ΔG^0(kcal/mol)	−7.11	−5.92	−6.36	
quercetin				
K_a (M^{-1})	6.73×10^3	1.7×10^4	1.04×10^4	0.04
r	0.06	0.12	0.12	
ΔG^0(kcal/mol)	−5.22	−5.77	−5.48	

[a]Association constant, K_a, ΔG^0, and fluorescence anisotropy r[b]. [b]λ_{ex} = 370 nm (350 nm for 3HF and 7HF), and λ_{em} = 530 nm for the anisotropy measurements. Standard free energy ΔG^0 was calculated using relation $\Delta G^0 = -RT \ln K_a$, where T = 298 K.

In duplex DNA solutions, the behavior of fisetin was very similar to that in G_4 (see Figure 2 and Table 1). The decrease in normal and increase in tautomer emission with increase in duplex DNA (I_T/I_N increased from 1.0 in buffer to 2.1 in 25 μM duplex) was associated with a red shift of the λ_{em}^{max} from 516 to 529 nm. However, the emission of 3HF dramatically changes in the duplex DNA. With a negligible change in normal emission, the tautomer emission increases rapidly with an increase in duplex DNA (I_T/I_N increased from 2.8 in buffer to 9.5 in 25 μM duplex) with a simultaneous red shift of the λ_{em}^{max} from 514 to 526 nm. The λ_{em}^{max} of quercetin changes from 529 in buffer to 536 nm with an increase in I_T/I_N from 1.3 to 3.24 in 25 μM duplex. No significant change for 7HF was observed in the duplex environment.

The situation in C_4 i-motif environment, however, is different from duplex and G_4 DNAs (see Table 1 and Figure 2). The most significant change was observed for 7HF, in which a blue shift in λ_{em}^{max} from 525 (in buffer) to 518 nm in 25 μM C_4 matrix occurred. It is to be noted that unlike 3HF and its derivatives fisetin and quercetin, in which the ESIPT is intrinsic (i.e., proceeding across an internal H-bond of the molecule) and barrier free,[46] the excited state proton transfer (ESPT) in 7HF (in which proton donor and acceptor sites are not located adjacent to each other) is solvent-assisted and consequently strongly depends on the nature of the solvent medium.[47] Time-resolved fluorescence spectroscopy and transient absorption measurements using two-step laser excitation (TSLE),[48] indicated that the ESPT of 7HF in methanol solution involves the formation of two types of phototautomers in the excited state as well as in the ground state. Both the blue and green fluorescence were due to the selective excitation of the same ground state species; namely, the conjugate anion of 7HF (7HFA). The fluorescence of 7HFA is strongly modulated by solvent relaxation owing to a large change in dipole moments between the ground and excited states of 7HFA.

Fluorescence anisotropy (r) measurements were also performed because this parameter serves as a sensitive indicator for monitoring ligand binding to macromolecular systems.[28,42,44] The anisotropy values of fluorophores are very low in fluid solution where the fluorophore molecules can freely rotate and increase in motionally constrained environments.[28] Table 2 presents the fluorescence anisotropy data obtained for the flavonoids in all the DNA environemnts. Higher values of r in DNA matrixes compared with buffer are indicative of the ligand (flavonoid)−receptor (DNA) adduct formation.

Measurements of Binding Parameters. Because the value of the binding constant gives an idea about the strength of the binding interactions and highlights the mode of binding, we have exploited the I_T/I_N titration data and the modified Benesi−Hildebrand equation[49] as follows to determine the binding constant (Figure 4) between the flavonoids and DNAs.

$$\frac{1}{\Delta\frac{I_T}{I_N}} = \frac{1}{n} + \frac{1}{nK_a[\mathrm{DNA}]} \quad (2)$$

Here, $\Delta(I_T/I_N) = |(I_T/I_{N_x}) - (I_T/I_{N_0})|$ where (I_T/I_{N_x}) and (I_T/I_{N_0}) represent the (I_T/I_N) of flavonoids in the presence and absence of DNA, respectively, n is the number of binding sites, and K_a is the association constant for the complex. A plot of $(1/\Delta(I_T/I_N))$ against $[\mathrm{DNA}]^{-1}$ gives a straight line where the ratio of intercept and slope provides the association constant, K_a. The association constants are given in Table 2. The number of binding sites were found to be 2.0, 2.0, and 0.4 for fisetin; 11.0, 2.0, and 1.0 for quercetin; and 2.0, 8.0, and 0.2 for 3HF in duplex, G_4, and C_4, respectively.

There are three ways a ligand can bind to DNA: (a) noncovalent, weak electrostatic interactions between cationic ligands and the polyanionic backbone of DNA; (b) intercalation between adjacent base pairs; and (c) hydrogen bonding interactions with the bases, which is mainly in the minor groove of DNA. However, a ligand can bind using more than one mechanism, which could be responsible for $n > 2$. The values of $n < 1$ is indicative of aggregation between the C_4 DNAs at higher concentrations. In B-form DNA, the minor

dx.doi.org/10.1021/jp508599h | J. Phys. Chem. B 2015, 119, 2546−2556

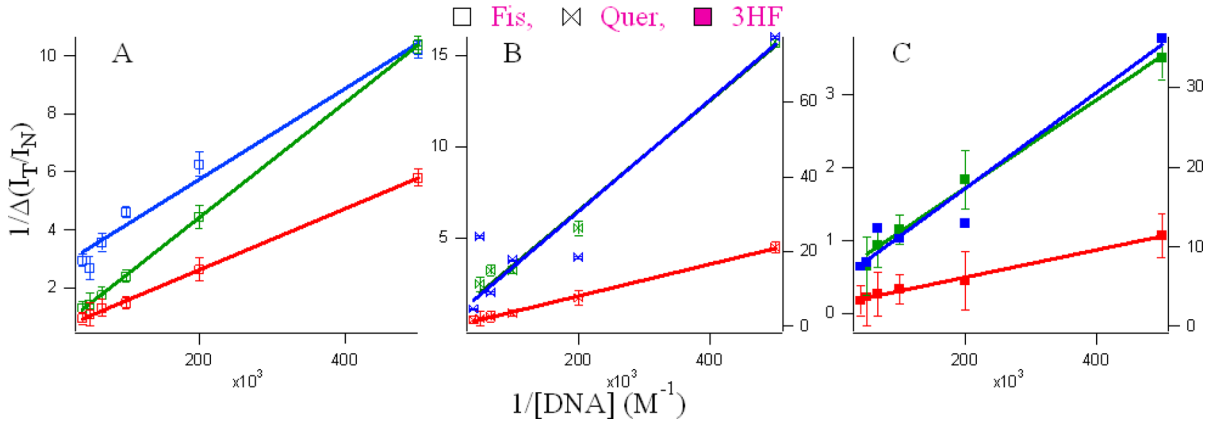

Figure 4. Double reciprocal plots using the I_T/I_N values from the spectral profiles of the flavonoids (A) fisetin, (B) quercetin and (C) 3HF in the various microenvironments of DNA (green, G_4; blue, C_4; and red, duplex).

groove is generally the preferred site of noncovalently binding ligands because binding is tighter in the narrower groove.[50] The association constants, K_a, for all the conjugates were obtained and are shown in Table 2. We observed weak binding for all the flavonoids in the order of 10^4–10^5 M^{-1} in the DNA, which agrees well with the literature for small molecule-DNA interactions.[51] The low association constants suggest that the binding of the flavonoids with their target DNA molecules takes place through noncovalent interactions either by intercalation or by groove/loop binding.

Size Exclusion Chromatographic (SEC) Measurements. To find out the nature of the free and conjugated quadruplex and duplex DNAs, SEC studies were carried out. Support for the existence of monomeric forms of C_4 and G_4 tetraplexes in $d(C_3TA_2)_3C_3$ and $d(T_2AG_3)_4$ oligonucleotides was obtained from molecular mass measurements (Figures 5 and SI Figure S4). Thymine oligonucleotides are used to relate observed retention times to molecular mass because these homo-oligonucleotides favor single-stranded and unfolded conformations. SEC with absorbance at 260 nm (see Figure 5) shows that the retention times of the free $d(C_3TA_2)_3C_3$, $d(T_2AG_3)_4$, and duplex are 10.65 (blue line), 10.41 (green line), and 9.81 (red line) minutes and the retention times of dT_5, dT_{12}, dT_{21}, dT_{24}, and dT_{30} were 11.22, 10.64, 10.16, 10.02, and 9.77 min, respectively (see Figure 5, top). With the intrinsic masses of the 21- ($d(C_3TA_2)_3C_3$) and 24-base-long ($d(T_2AG_3)_4$) oligonucleotides of 6200 and 7575 g/mol, the retention times in SEC should have been around dT_{21} (6326 g/mol) and dT_{24}, (7239 g/mol), which were not observed from the experiments. This was indicative of the folded nature of $d(C_3TA_2)_3C_3$ and $d(T_2AG_3)_4$ in the solution, making it behave as a smaller sized oligonucleotide (such as dT_{12} and dT_{14}).

To study the size and shape of the flavonoid-DNA adducts through the tautomer fluorescence in SEC, we chose to study fisetin with duplex DNA as the representative of all adducts because fisetin undergoes significant ESIPT upon binding with the duplex with an appreciably high K_a. Figure 5, bottom, displays the SEC profiles of fisetin bound to the duplex of $d(C_3TA_2)_3C_3$ and $d(T_2AG_3)_4$ using absorbance at 370 nm (red - - -) and fluorescence at 530 nm (λ_{ex} = 370 nm, red —·—·—) with a retention time of 9.68 min, whereas the free duplex eluted at 9.81 min (red —, studied by A_{260}). The presence of fisetin in the duplex made it larger, making its retention time less than the free duplex (Figure 5 bottom). Relative to the linear fit of the plot of the retention time vs molecular masses

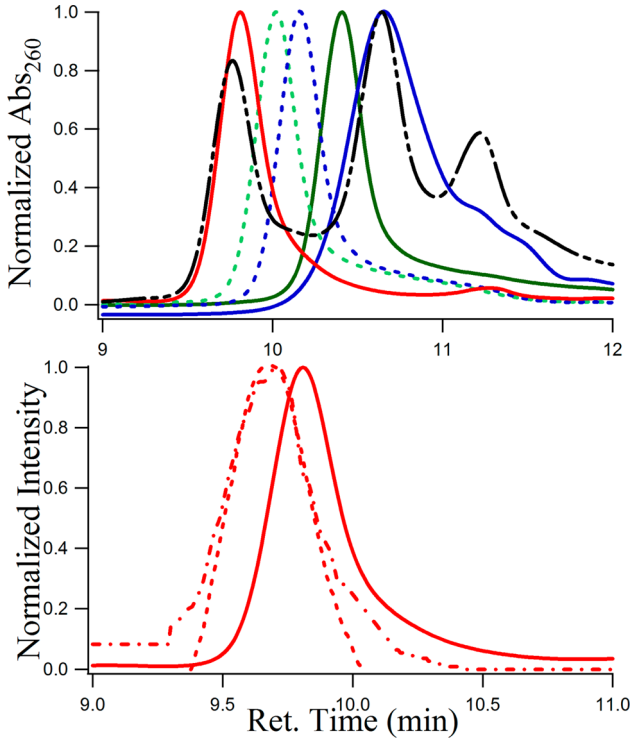

Figure 5. Size-exclusion chromatograms of (top) 5 μM solutions of $d(C_3TA_2)_3C_3$ (blue —), $d(T_2AG_3)_4$ (green —), duplex of $dC_3TA_2)_3C_3$/$d(T_2AG_3)_4$ (red —), a mixture of dT_5, dT_{12}, and dT_{30} (black — - - —), dT_{21} (blue dashed - - -), dT_{24} (green dashed - - - oligonucleotides studied by absorbance at 260 nm. (bottom) Fisetin conjugated duplex, where (- - -) and (—·—) respectively denote λ_{abs} at 370 nm, λ_{em} = 530/λ_{em} = 370 along with free duplex (— —) with λ_{abs} = 260 nm. The time difference of 0.06 min between the fluorescence and absorption due to the time lag between the two detectors (see the Materials and Methods section[29]) is corrected here.

of single-stranded thymine oligonucleotides (SI Figure S4), the calculated molecular masses for free and fisetin-bound duplex $d(C_3TA_2)_3C_3/d(T_2AG_3)_4$ are found to be 8526 and 9158 g/mol, with a difference of 632 g/mol. It is noteworthy that the molar mass of fisetin is 286.24 g/mol, which strongly indicates that the binding stiochiometry between $d(C_3TA_2)_3C_3$/d-$(T_2AG_3)_4$ and fisetin should be 1:2. This agrees very well with the fluorescence spectroscopic measurements in which the number of binding sites (n) of fisetin in duplex DNA was found

dx.doi.org/10.1021/jp508599h | J. Phys. Chem. B 2015, 119, 2546–2556

to be 2 (see above). Thus, although the optical spectroscopic measurements indicated the nature of the secondary structures (C_4, G_4, duplex) of the C-rich and G-rich and their duplex DNA molecules along with the mode of noninvasive binding of flavonoids with the DNAs, SEC studies support the quantitative aspect of this study. For fisetin conjugated C_4 i-motif and G_4 quadruplex DNAs, we observed a high degree of aggregation in the SEC profiles, the origin of which is unclear to us at this point.

Displacement Studies. To understand the mode of binding of the flavonoids in the DNA environments, we have exploited the well known extrinsic fluorescence probe ethidium bromide (EtBr), which mostly intercalates in DNA.[52] For duplex DNA, ligands bind mainly through intercalation or as a groove binder. However, for quadruplex DNA, ligands can intercalate or bind to the loops (see Scheme 2, where straight arrows indicate the loops and grooves). Literature data provide evidence that EtBr binds with quadruplex mainly through intercalation or end stacking modes.[52] The solid line (— profile 1) in Figure 6 indicates the emission intensities of fisetin in the DNA in the presence of EtBr. The I_T/I_N of 5 μM fisetin in the presence of 5 μM EtBr is 1.43, 1.75, and 1.7 in 10 μM C4, G4, and duplex, respectively, which suggests that in the presence of EtBr, there was not a major decrease in fluorescence emission of fisetin (see Table 1 for comparison).

Scheme 2. Schematic Diagram of the Duplex (top) Made up of Single-Stranded Oligonucleotides 5′-d(C_3TA_2)$_3C_3$-3′ and 5′-d(T_2AG_3)$_4$-3′ and the Unusual Tetraplex (bottom) Secondary Structures, Namely, C_4 i-Motif[a] and Antiparallel G_4-Quadruplex[b] Structures[c]

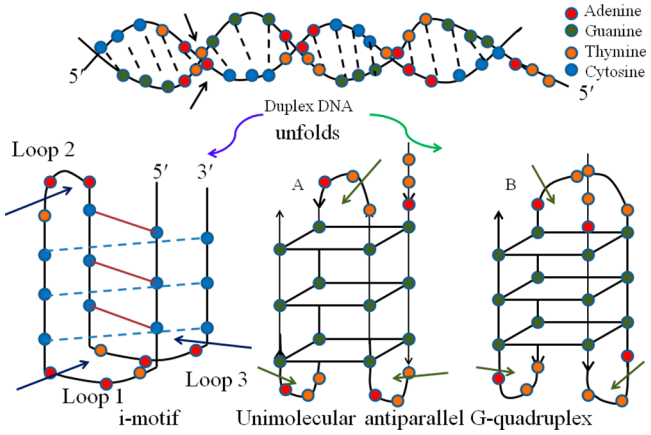

[a]Left, formed by 5′-d(C_3TA_2)$_3C_3$-3′. [b]Right, made up by 5′-d(T_2AG_3)$_4$-3′. [c]A and B denote the unimolecular antiparallel structure with parallel adjacent strands and a diagonal loop and unimolecular antiparallel with alternating parallel strands, respectively. The straight arrows indicate the site of binding of flavonoids in the DNA matrix. The bindings sites are groove and loop for duplex and quadruplex DNAs, respectively.

The black emission profiles in Figure 6 correspond to the fluorescence emission spectra of 5 μM EtBr in buffer (black ····), in 10 μM C_4, G_4, and duplex DNA in the absence (profile 2, —··—) and presence (profile 3, — —) of 5 μM fisetin. As is evident from Figure 6, the fluorescence of EtBr increases significantly (8.5, 4, 1.6 times for duplex, G_4 and for C_4, respectively) upon binding with DNA. There is a slight increase in the emission intensity of EtBr in DNA matrixes in the presence of fisetin. Furthermore, the process of energy transfer[20,26,28,44,45] was readily observed from the excitation spectrum of the EtBr in the presence of fisetin. The pink (profile 4, - - -) and black (profile 5, —··—··—) lines in Figure 6 show the fluorescence excitation of EtBr (λ_{em} = 610 nm) in 10 μM DNA in the absence and presence of fisetin, and the appearance of a band at 370 nm only in the latter case clearly indicates the existence of both fisetin and EtBr in the DNA matrix and the occurrence of FRET from fisetin to the intercalated EtBr.

The energy transfer from fisetin to EtBr increases the emission intensity of EtBr to a slight extent in the presence of fisetin (compare profiles 4 and 5 in each DNA environments). This suggests that fisetin and EtBr bind with the DNA at the same time. This can be true only if their binding sites are different, but are adjacent to each other in d(C_3TA_2)$_3C_3$, d(T_2AG_3)$_4$, and duplex DNAs, which makes the FRET from fisetin to EtBr possible. For quercetin, we observed a similar energy transfer mechanism (see SI Figure S5) in the G_4 environment; however, because the intrinsic fluorescence of quercetin is less than fisetin, the energy transfer from quercetin to EtBr became prominent in all the DNA environments because with λ_{ex} = 370 nm, apart from emission from normal at λ_{em} ~ 470 nm (low) and ESIPT at λ_{em} ~ 530 nm, a third emission is observed at λ_{em} ~ 592 nm, which is the intrinsic λ_{em}^{max} for EtBr.[52] Hence, the energy from the emission of the normal species at 470 nm is transferred to excite the EtBr, giving rise to the EtBr emission band in the spectrum. This mechanism is also present in the case of fisetin, but because of the high intrinsic fluorescence and broadness of the emission spectrum, it was not noticeable. These observations clearly indicate that fisetin and quercetin bind at sites that are in close

Table 3. Binding Parameters for 3HF, 7HF, Fisetin, Quercetin in C_4 i-Motif, G_4 Quadruplex, and Duplex DNAs Analyzed from Computational Docking Studies Using the AutoDockTools4 Program

binding parameters from docking studies	C_4 i-motif	antiparallel-G_4	duplex B-DNA	A-DNA
		Binding Energy (kcal/mol)		
3-HF	−5.25	−6.93	−7.06	−8.47
7-HF	−5.83	−6.43	−7.84	−8.95
fisetin	−5.64	−6.66	−7.38	−9.03
quercetin	−6.27	−6.39	−7.19	−8.91
		K_a (M^{-1})		
3-HF	7.09×10^{04}	1.19×10^{05}	1.49×10^{05}	1.67×10^{06}
7-HF	1.88×10^{05}	5.18×10^{04}	5.56×10^{05}	3.33×10^{06}
fisetin	1.35×10^{05}	7.63×10^{04}	2.56×10^{05}	5.00×10^{06}
quercetin	3.97×10^{05}	4.83×10^{04}	1.89×10^{05}	3.33×10^{06}

dx.doi.org/10.1021/jp508599h | J. Phys. Chem. B 2015, 119, 2546−2556

Table 4. Internal Energy[a] for 3HF, 7HF, Fisetin, Quercetin in the C_4 i-Motif, G_4 Quadruplex, and Duplex DNAs Analyzed from Computational Docking Studies Using the AutoDockTools4 Program

DNA	C_4		G_4		B-DNA		A-DNA	
int. energy (kcal/mol)	ES	vdw−hb	ES	vdw−hb	ES	vdw−hb	ES	vdw−hb
3HF	0.08	5.77	0.25	7.28	0	7.66	0.02	9.09
7HF	0.38	6.05	0.27	6.75	0.04	8.4	0.1	9.45
fisetin	0.36	6.76	0.59	7.56	0.13	8.74	0.13	10.4
quercetin	0.75	7.32	0.51	7.67	0.17	8.81	0.13	10.57

[a]Sum of electrostatic (ES) and van der Waals−H-bond desolvation (vdw−hb) (kcal/mol).

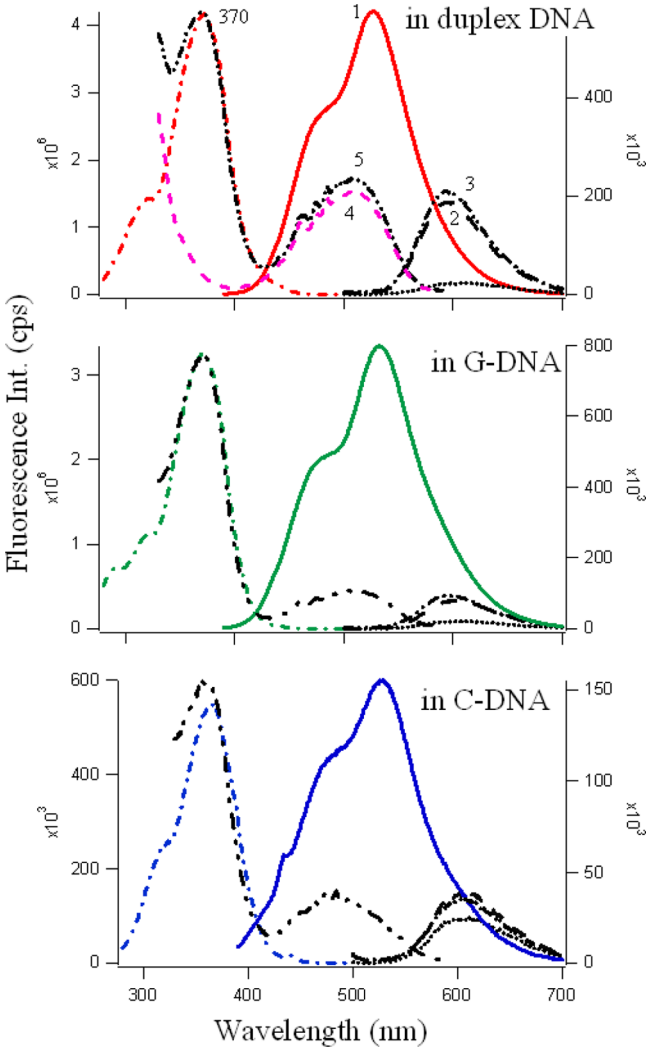

Figure 6. Fluorescence emission (solid line, profile 1) and excitation spectra (—·—) of 5 μM fisetin (λ_{ex} = 370 nm) in 10 μM DNA (C_4 (blue), G_4 (green) and duplex (red)) in the presence of 5 μM EtBr. The black profiles correspond to emission of 5 μM EtBr (λ_{ex} = 480 nm) in buffer (····), in DNA (10 μM, — —, in the absence of fisetin, profile 2), and in DNA (10 μM, —·—, in the presence of 5 μM fisetin, profile 3). The figure also shows the excitation spectra of EtBr (λ_{em} = 610 nm) in DNA without (pink - - -, profile 4) and with (black —··—··—, profile 5) fisetin. Profile numbers are not repeated for G and C DNAs, but they correspond to the same sets in each.

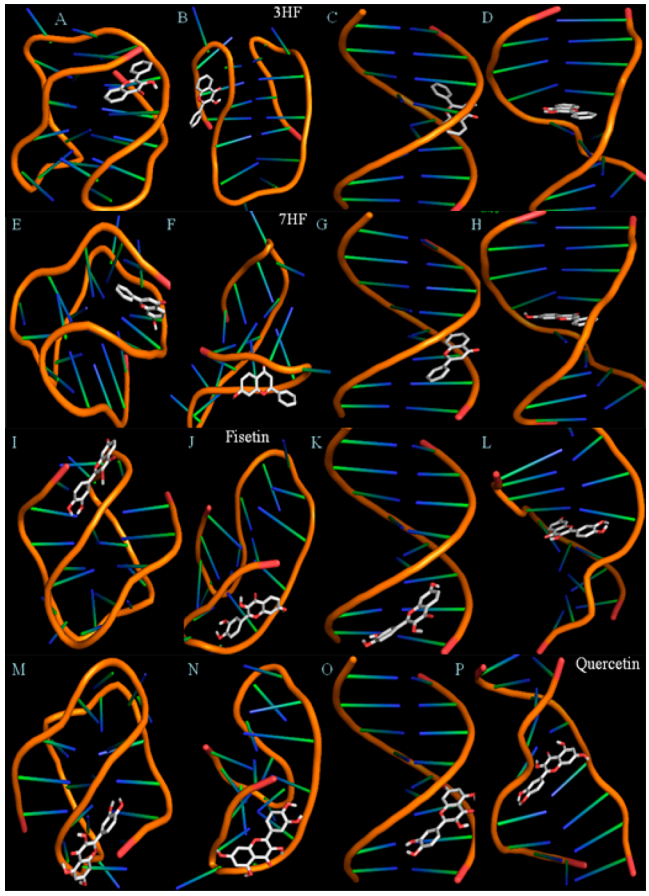

Figure 7. Lowest-energy-docked conformations representing the interaction profile of 3-hydroxyflavone (3HF, A−D), 7-hydroxyflavone (7HF, E−H), fisetin (I−L) and quercetin (M−P) in antiparallel C_4 i-motif, antiparallel G_4 quadruplex, B-DNA, and A-DNA (left to right). The binding parameters are given in Tables 3 and 4.

proximity to the intercalated EtBr for energy transfer to take place. Therefore, possible binding sites for fisetin and quercetin were the loop regions of C_4; the face of the G-quartet along the diagonal loop (see Scheme 2), where π-delocalized system stacking is possible; and the minor groove of duplex DNA.[53,54]

Molecular Docking Studies. Molecular modeling studies enable characterization of DNA−flavonoid interactions in atomistic detail. Molecular docking techniques have come into prominence as a new tool for identifying novel small molecule drugs for targeting DNA.[55,56] Figure 7 displays the lowest-energy-docked conformers for 3HF, 7HF, fisetin, and quercetin in C_4, G_4, and duplex DNAs. All the flavonoids were found to be either loop or minor groove binders for quadruplex or duplex, respectively. The minor groove is a particularly attractive target for small molecules because of the closer proximity of the strands in the minor groove, thereby making the binding more compact.[57] Furthermore, this site has less competition from proteins and polymerases, which typically interact with the major groove.[58] Table 3 provides the binding energies and association constants for 3-hydroxyflavone (3HF),

dx.doi.org/10.1021/jp508599h | J. Phys. Chem. B 2015, 119, 2546−2556

7-hydroxyflavone (7HF), fisetin, quercetin in C_4 i-motif, G_4 quadruplex, and duplex B- and A-DNA environments, which were obtained using the AutoDockTools4 program. The flavonoids intercalate with A-DNA, for which the average K_a was found to be $\sim 10^6$ (which is at least 1 order of magnitude higher than other DNAs) and the average binding energy was ~9 kcal/mol (vs ~6−7 kcal/mol in other DNAs). A comparison between the computational and experimental binding energies and association constants reveals that theoretical and experimental results do match to an appreciable extent. However, there were some discrepancies observed that could be due to a higher order of aggregation of both ligands (flavonoids) and receptors (DNAs) in the solutions.

Table 4 provides the internal energy of the ligand flavonoids in their host DNA environments. The internal energy is the sum of electrostatic and van der Waals−H-bonding desolvation energy. Hence, higher internal energy arises from more association of the ligand with the host. Fisetin and quercetin form H bonds to their receptor DNA environments through the C(3′)−OH, C(4′)−OH in B, and C(7)−OH in the A rings. The C(5)−OH of quercetin can interact with the host only when it no longer interferes with the ESIPT.[44,45] The C(3)−OH in fisetin, quercetin, and 3HF forms H bonds with its host when ESIPT does not occur or when the microenvironment is not aprotic.[26,42] On the other hand, ESIPT in 7HF happens only via H bonding with its receptor/surrounding environment.

CONCLUSIONS

The high sensitivity of flavonol emission to their surrounding environment and their prospective applications as exquisitely sensitive fluorescent molecular probes for exploring their interactions with the biological targets were the focus of this study. Here, we presented perspectives highlighting the novel uses of the intrinsic fluorescence emission of the therapeutically potent flavonoids quercetin and fisetin and their chromophores 3HF and 7HF in exploring their interactions with the DNA oligonucleotides of physiological relevance. Applying this promising new approach for the "screening" and "design" of the most suitable derivatives from among numerous available structural variants of this new generation of therapeutic drugs would open the door to new avenues in medicinal chemistry. Complementary use of other experimental biophysical (spectroscopic as well as chromatographic) techniques and theoretical (molecular modeling) studies permits detailed assessment of the role of structure and substitution patterns of the flavonoids on their affinities and binding modes to their target DNAs.

ASSOCIATED CONTENT

Supporting Information

Figures S1−S5. This material is available free of charge via the Internet at http://pubs.acs.org.

AUTHOR INFORMATION

Corresponding Author

*Phone: +1-601-977-7779. Fax: +1-601-977-7898. E-mail: bsengupta@tougaloo.edu; bsgupta.tougaloo@gmail.com.

Notes

The authors declare no competing financial interest.

ACKNOWLEDGMENTS

This work was supported by the Mississippi INBRE, funded by an Institutional Development Award (IDeA) from the National Institute of General Medical Sciences of the National Institutes of Health under Grant No. P20GM103476. B.S.G. also acknowledges financial and research support from NSF MS-EPSCoR Grant No. EPS-0903787, NIH/NCMHHD/RIMI Grant No. 1P20MD002725, HHMI Grant No. 52007562, Jackson Heart Study program with the Contract No. N01-HC-95172 at Tougaloo College. We are especially grateful to Professor Wolfgang Kramer for his invaluable help in data collection using the CD spectrometer at Millsaps College, Jackson, MS. Undergraduate chemistry majors D.D., K.H., and biology majors D.W., D.G., C.H. thank their respective departments at TC. R.W. and S.R. are supported by NIH award 1R15CA173667-01A1.

REFERENCES

(1) Harborne, J. B. In *Plant Flavonoids in Biology and Medicine II: Biochemical, Cellular and Medicinal properties*; Cody, V.; Middleton, E.; Harborne, J. B.; Beretz, A. Eds.; Alan R. Liss: New York, 1988.

(2) Rusznyák, St.; Szent-Györgyi, A. Vitamin P: flavonols as vitamins. *Nature* **1936**, *138*, 27−27.

(3) Mulligan, A. A.; Welch, A. A.; McTaggart, A. A.; Bhaniani, A.; Bingham, S. A. Intakes and sources of soya foods and isoflavones in a UK population cohort study (EPIC-Norfolk). *Eur. J. Clin. Nutr.* **2007**, *61*, 248−254.

(4) Renaud, S.; de Lorgeril, M. Wine, alcohol, platelets, and the French paradox for coronary heart disease. *Lancet* **1992**, *339*, 1523−1526.

(5) Kris-Etherton, P. M.; Keen, C. L. Evidence that the antioxidant flavonoids in tea and cocoa are beneficial for cardiovascular health. *Curr. Opin. Lipidol.* **2002**, *13*, 41−9.

(6) Nair, M. P.N.; Saiyed, Z. M.; Gandhi, N. H.; Ramchand, C. N. The flavonoid, quercetin, inhibits HIV-1 infection in normal peripheral blood mononuclear cells. *Am. J. Infect. Dis.* **2009**, *5*, 135−141.

(7) Harborne, J. B.; Williams, C. A. Advances in flavonoid research since 1992. *Phytochemistry* **2000**, *55*, 481−504.

(8) Zheng, L. T.; Ock, J.; Kwon, B. M.; Suk, K. Suppressive effects of flavonoid fisetin on lipopolysaccharide-induced microglial activation and neurotoxicity. *Int. Immunopharmacol.* **2008**, *8*, 484−94.

(9) Mariní, M.; Piantanida, I.; Rusak, G.; Zini, M. Interactions of quercetin and its lanthane complex with double-stranded DNA/RNA and single-stranded RNA. Spectrophotometric sensing of poly G. *J. Inorg. Biochem.* **2006**, *100*, 288−298.

(10) Boyle, S. P.; Dobson, V. L.; Duthie, S. J.; Kyle, J. A. M.; Collins, A. R. Absorption and DNA protective effects of flavonoid glycosides from an onion meal. *Eur. J. Nutr.* **2000**, *39*, 213−223.

(11) Ragazzon, P. A.; Bradshaw, T.; Matthews, C.; Iley, J.; Missailidis, S. The characterization of flavone-DNA isoform interactions as a basis for anticancer drug development. *Anticancer Res.* **2009**, *29*, 2273−83.

(12) Greider, C. W.; Blackburn, E. H. Identification of a specific telomere terminal transferase activity in tetrahymena extracts. *Cell* **1985**, *43*, 405−413.

(13) O'Connor, C. Telomeres of Human Chromosomes. *Nat. Educ.* **2008**, *1*, 166−166.

(14) Mirkin, S. M. Discovery of alternative DNA structures: A heroic decade (1979−1989). *Front. Biosci.* **2008**, *13*, 1064−1071.

(15) Sen, D.; Gilbert, W. Formation of parallel four-stranded complexes by guanine-rich motifs in DNA and its applications for meiosis. *Nature* **1988**, *334*, 364−366.

(16) Phan, A. T.; Guéron, M.; Leroy, J. L. The solution structure and internal motions of a fragment of the cytidine-rich strand of the human telomere. *J. Mol. Biol.* **2000**, *299*, 123−144.

(17) Biffi, G.; Tannahill, D.; McCafferty, J.; Balasubramnium, S. Quantitative visualization of DNA G-quadruplex structures in human cells. *Nat. Chem.* **2013**, *5*, 182−186.

(18) Eddy, J.; Maizels, N. Gene function correlates with potential for G4 DNA formation in the human genome. *Nucleic Acids Res.* **2006**, *34*, 3887−3896.
(19) Granotier, C.; Pennarun, G.; Riou, L.; Hoffschir, F.; Gauthier, L. R.; Cian, A. D.; Gomez, D.; Mandine, E.; Riou, J. F.; Mergny, J. L.; Mailliet, P.; Dutrillaux, B.; Boussin, F. D. Preferential binding of a G-quadruplex ligand to human chromosome ends. *Nucleic Acids Res.* **2005**, *33*, 4182−4190.
(20) Sengupta, B.; Pahari, B.; Blackmon, L.; Sengupta, P. K. Prospect of bioflavonoid fisetin as a quadruplex DNA ligand: A biophysical approach. *PLoS One* **2013**, *8*, e65383 DOI: 10.1371/journal.-pone.0065383.
(21) Pandey, R. P.; Parajuli, P.; Koirala, N.; Park, J. W.; Sohng, J. K. Probing 3-Hydroxyflavone for in vitro glycorandomization of flavonols by YjiC. *Appl. Environ. Microbiol.* **2013**, *79*, 6833−6838.
(22) Matter, W. F.; Brown, R. F.; Vlahos, C. The inhibition of phosphatidylinositol 3-kinase by quercetin and analogs. *Biochem. Biophys. Res. Commun.* **1992**, *186*, 624−631.
(23) Boege, F.; Straub, T.; Kehr, A.; Boesenberg, C.; Christiansen, K.; Andersen, A.; Jakob, F.; Kohrle, J. Selected novel flavones inhibit the DNA binding or the DNA religation step of eukaryotic topoisomerase I. *J. Biol. Chem.* **1996**, *271*, 2262−2270.
(24) Ferricola, P. C.; Cody, V.; Middleton, E. Protein kinase C inhibition by plant flavonoids: Kinetic mechanisms and structure−activity relationships. *Biochem. Pharmacol.* **1989**, *381*, 1617−1624.
(25) Brinkworth, R. S.; Stoermer, M. J.; Fairlie, D. P. Flavones are inhibitors of HIV-1 proteinase. *Biochem. Biophys. Res. Commun.* **1992**, *188*, 631−637.
(26) Sengupta, B.; Banerjee, A.; Sengupta, P. K. Investigations on the binding and antioxidant properties of the plant flavonoid fisetin in model biomembranes. *FEBS Lett.* **2004**, *570*, 77−81.
(27) Sengupta, B.; Swenson, J. Properties of normal and glycated human hemoglobin in presence and absence of antioxidant. *Biochem. Biophys. Res. Commun.* **2005**, *334*, 954−959.
(28) Lakowicz, J. R. *Principles of Fluorescence Spectroscopy*, 3rd ed.; Springer: New York, 2006; http://www.springer.com/978-0-387-31278-1.
(29) Sengupta, B.; Springer, K.; Buckman, J.; Story, S. P.; Abe, O. H.; Hasan, Z. W.; Prudowsky, Z. D.; Rudisill, S. E.; Degtyareva, N. N.; Petty, J. T. DNA templates for fluorescent silver clusters and i-motif folding. *J. Phys. Chem. C* **2009**, *113*, 19518−19524.
(30) Morris, G. M.; Huey, R.; Lindstrom, W.; Sanner, M. F.; Belew, R. K.; Goodsell, D. S.; Olson, A. J. Autodock4 and AutoDockTools4: Automated docking with selective receptor flexiblity. *J. Comput. Chem.* **2009**, *30*, 2785−2791.
(31) Morris, G. M.; Huey, R.; Olsonm, A. J. Using autodock for ligand-receptor docking. *Curr. Protoc. Bioinform.* **2008**, *24*, 8−14.
(32) Pettersen, Eric F.; et al. UCSF Chimera—a visualization system for exploratory research and analysis. *J. Comput. Chem.* **2004**, *25*, 1605−1612.
(33) Wang, Y.; Patel, D. J. Solution structure of the human telomeric repeat d[$AG_3(T_2AG_3)_3$] G-tetraplex. *Structure* **1993**, *1*, 263−282.
(34) Han, X.; Leroy, J. L.; Guéron, M. An intramolecular i-motif: The solution structure and base-pair opening kinetics of d-($5mCCT_3CCT_3ACCT_3CC$). *J. Mol. Biol.* **1998**, *278*, 949−965.
(35) Kamitori, S.; Takusagawa, F. Multiple binding modes of anticancer drug actinomycin D: X-ray, molecular modeling, and spectroscopic studies of d (GAAGCTTC) 2-actinomycin D complexes and its host DNA. *J. Am. Chem. Soc.* **1994**, *116*, 4154−4165.
(36) Arnott, S.; Hukins, D. Optimised parameters for A-DNA and B-DNA. *Biochem. Biophys. Res. Commun.* **1972**, *47*, 1504−1509.
(37) Mergny, J.-L.; Li, J.; Lacroix, L.; Amrane, S.; Chaires, J. B. Thermal difference spectra: A specific signature for nucleic acid structures. *Nucleic Acids Res.* **2005**, *33*, 138−142.
(38) Fernández, S.; Eritja, R.; Avīnó, A.; Jaumota, J.; Gargallo, R. Influence of pH, temperature and the cationic porphyrin TMPyP4 on the stability of the i-motif formed by the 5′-(C3TA2)4-3′ sequence of the human telomere. *Int. J. Biol. Macromol.* **2011**, *49*, 729−736.
(39) Vorlickova, M.; Kejnovska, I.; Bednarova, K.; Rencuik, D.; Kypr, J. Circular dichroism spectroscopy of DNA: From duplexes to quadruplexes. *Chirality* **2012**, *24*, 691−698.
(40) Phan, A. T.; Leroy, J. L. Intramolecular i-Motif Structures of Telomeric DNA. *J. Biomol Struct. Dyn.* **2000**, *17*, 245−51.
(41) Sengupta, P. K.; Kasha, M. Excited state proton-transfer spectroscopy of 3-hydroxyflavone and quercetin. *Chem. Phys. Lett.* **1979**, *68*, 382−385.
(42) Guharay, J.; Dennison, S. M.; Sengupta, P. K. Influence of different environments on the excited-state proton transfer and dual fluorescence of fisetin. *Spectrochim. Acta, Part A* **1999**, *55*, 1091−1099 and references cited therein.
(43) Kasha, M. Proton-transfer spectroscopy: Perturbation of the tautomerization potential. *J. Chem. Soc. Faraday Trans 2* **1986**, *82*, 2379.
(44) Sengupta, B.; Sengupta, P. K. The interaction of quercetin with human serum albumin: A fluorescence spectroscopic study. *Biochem. Biophys. Res. Commun.* **2002**, *299*, 400−403.
(45) Sengupta, B.; Sengupta, P. K. Binding of quercetin with human serum albumin: A critical spectroscopic study. *Biopolymers (Biospectroscopy)* **2003**, *72*, 427−434.
(46) Kasha, M. Proton transfer spectroscopy and proton-transfer lasers. *Acta Phys. Pol., A* **1987**, *71*, 717−729.
(47) Sengupta, B.; Guharay, J.; Sengupta, P. K. Reverse micelles of TX-100 in mixed solvents of benzene and *n*-hexane: Fluorescence studies using 7HF as probe. *J. Surf. Sci. Technol.* **1998**, *14*, 150−156.
(48) Itoh, M.; Adachi, T. Transient absorption and two-step laser excitation fluorescence studies of the excited-state proton transfer and relaxation in the methanol solution of 7-hydroxyflavone. *J. Am. Chem. Soc.* **1984**, *106*, 4320−4324.
(49) Pahari, B.; Sengupta, B.; Chakraborty, S.; Thomas, B.; McGowan, D.; Sengupta, P. K. Contrasting binding of fisetin and daidzein in γ-cyclodextrin nanocavity. *J. Photochem. Photobiol. B* **2013**, *118*, 33−41.
(50) Beck, J. L.; Colgrave, M. L.; Ralph, S. F.; Sheil, M. M. Electrospray ionization mass spectrometry of oligonucleotide complexes with drugs, metals, and proteins. *Mass Spectrom. Rev.* **2001**, *20*, 61−87.
(51) Sirajuddin, M.; Ali, S.; Badshah, A. Drug−DNA interactions and their study by UV−Visible, fluorescence spectroscopies and cyclic voltametry. *J. Photochem. Photobiol. B* **2013**, *124*, 1−19.
(52) Guo, Q.; Lu, M.; Marky, L. A.; Kallenbach, N. R. Interaction of the dye ethidium bromide with DNA containing guanine repeats. *Biochemistry* **1992**, *31*, 2451−2455.
(53) Neidle, S. The structures of quadruplex nucleic acids and their drug complexes. *Current Opin. Struct. Biol.* **2009**, *19*, 239−250.
(54) Ji, X.; Sun, H.; Zhou, H.; Xiang, J.; Tang, Y.; Zhao, C. The interaction of telomeric DNA and C-myc22 G-quadruplex with 11 natural alkaloids. *Nucleic Acid Therapeutics* **2012**, *22*, 127−136.
(55) Hurley, L. H. Secondary DNA structures as molecular targets for cancer therapeutics. *Biochem. Soc. Trans.* **2001**, *29*, 692−696.
(56) Detering, C.; Varani, G. Validation of automated docking programs for docking and database screening against RNA drug targets. *J. Med. Chem.* **2004**, *47*, 4188−4201.
(57) Reddy, B. S.; Sondhi, S. M.; Lown, J. W. Synthetic DNA minor groove-binding drugs. *Pharmacol. Ther.* **1999**, *84*, 1−111.
(58) Tse, W. C.; Boger, D. L. Sequence-selective DNA recognition: Natural products and nature's lessons. *Chem. Biol.* **2004**, *11*, 1607−1617.